Journal of Magnetic Resonance 198 (2009) 167–173

Contents lists available at ScienceDirect

Journal of Magnetic Resonance

journal homepage: www.elsevier.com/locate/jmr

Observation of molecular migration in porous media using 2D exchange spectroscopy in the inhomogeneous magnetic field

Lauren M. Burcaw, Paul T. Callaghan *

MacDiarmid Institute for Advanced Materials and Nanotechnology, School of Chemical and Physical Sciences, Victoria University of Wellington, New Zealand

ARTICLE INFO

Article history:
Received 16 December 2008
Revised 2 February 2009
Available online 6 March 2009

Keywords:
Diffusion
Porous media
2D exchange
Inhomogeneous fields

ABSTRACT

We present a new method for observing fluid diffusion in a porous medium. The method employs 2D exchange spectroscopy for molecules diffusing in the presence of local magnetic field inhomogeneities, in our case distilled water in various sized glass bead packs. Our experiment involves an acquisition and evolution time domain with the two Fourier domains corresponding to the spectral distribution of local fields. We show that exchange in the internal magnetic field can be seen in a 2D spectrum with a characteristic time on the order of that required to diffuse 0.15 sphere diameters with similar behavior found for computer simulations. The method is potentially useful for studying the internal migrations in more complicated systems such as sandstones or other porous media.

1. Introduction

One of the important questions in porous media physics concerns the rate at which imbibed fluid molecules diffuse from pore to pore. In petrophysics, this is particularly relevant as it bears on the question of rock permeability. A number of NMR methods allow for an investigation of fluid diffusion. Pulsed Gradient Spin Echo NMR [1] allows for a direct measurement of molecular translational motion as do spin echo experiments in which one observes signal attenuation due to diffusion in the locally inhomogeneous magnetic field [2]. Recently a two-dimensional T_2 exchange method has been proposed [3,4] in which one labels molecules in a local pore by virtue of the pore size dependent T_2 value. Being an exchange method, the technique senses changes in T_2 values as evidenced by the growth of off-diagonal intensity following a mixing time during which molecules are allowed to diffuse. This method relies on the use of two-dimensional Laplace inversion [5] and is one of a number of 2D separation, correlation and exchange methods [6,3,7–11] based on this type of analysis. However, there are difficulties associated with the inverse Laplace Transform because of pearling effects [12]. This can lead to some ambiguity when it comes to interpreting peak locations. Kuntz et al. [13] have proposed a new 2D exchange experiment which involves only the Fourier transformation. This simple exchange method in principle allows one to investigate exchange between pores of imbibed fluid molecules, simply as a result of changes in local Larmor frequencies.

It is well known that porous media in an applied magnetic field will experience internal magnetic field inhomogeneities due to susceptibility differences between the matrix and the pore space. The magnetic field variations will in turn give rise to an inhomogeneous broadening of the NMR lineshape. Such local field inhomogeneity was investigated many years ago by Brown [14] using ferromagnetic grains suspended in water with 5% carboxy-methylcellulose, and expanded upon by Drain [15] who examined the broadening of magnetic resonance lines in powdered samples. More recently, the internal field has been studied in more depth by Audoly et al. [16] using a Finney pack of non-penetrating spheres. They find that the variation of the internal magnetic field occurs over the length scale of the pore size in the bead pack, and that its distribution is approximately symmetrical due to the superposition of the field from multiple spheres. Chen et al. [17] simulate the internal magnetic field for both a fully and partially water saturated Berea sandstone and find similar results to Audoly et al.

Consider water molecules distributed through the pore space of a porous medium placed in an external magnetic field. As these molecules diffuse, they will experience fluctuations in the local internal magnetic fields arising from inhomogeneities caused by the magnetic susceptibility difference of the matrix and water. For frequency-encoding times that are small compared with the time to diffuse a significant distance in the pore geometry, the 1D spectrum is characteristic of the inhomogeneously broadened line associated with the static distribution of molecule locations. Of course the characteristic time is here associated with the frequency spread associated with the inhomogeneous linewidth, $\tau_c^{-1} \sim \delta\omega$. Hence, motional narrowing will occur when the characteristic length, l, over which a representative variation of magnetic

* Corresponding author. Fax: +64 6 350 5164.
E-mail address: paul.callaghan@vuw.ac.nz (P.T. Callaghan).

1090-7807/$ - see front matter © 2009 Elsevier Inc. All rights reserved.
doi:10.1016/j.jmr.2009.02.009

field is found, is such that $l^2\delta\omega/D \ll 1$, where D is the self diffusion coefficient of the liquid molecule. In the slow motion limit, $l^2\delta\omega/D \gg 1$, frequency encoding of spins gives a good sense of spatial location. By contrast in the fast motion case, spatial localisation is lost. This means that the experiment we propose works best for large field inhomogeneity and/or large pores. However, as we shall show here, even when the slow motion condition is relaxed, good estimates of pore–pore exchange times can be made.

The recent work of Kuntz et al. involved a polydisperse glass bead pack in which significant exchange occurred during the frequency encoding time. In the present paper we extend that work to investigate frequency exchange in a monodisperse glass bead pack and using a B_0 up to 21 T (900 MHz), thus ensuring the criterion $l^2\delta\omega/D \ll 1$.

2. Method

In an exchange experiment we seek to monitor the migration of molecules to different field positions. This is done by using a pulse sequence similar to a NOESY [18] with two independent frequency-encodings, t_1 and t_2, separated by a mixing time. Ideally the frequency encoding times will be short compared to the mixing period. Fig. 1 shows the relevant sequence.

An initial excitation 90° pulse rotates the magnetization to the transverse plane. After an evolution time, t_1, a second storage 90° pulse brings the magnetization back to the z-axis. This inhibits T_2 relaxation, although the magnetization will still experience T_1 relaxation. Following this storage pulse, we wait a mixing time τ_m, and then apply the third 90° pulse which rotates the magnetization back to the transverse plane. We then acquire signal over a sampling time labelled t_2. Phase cycling is used to ensure that the only signal obtained is from that transverse magnetisation which derived from the initial 90° excitation pulse.

This pulse sequence is repeated n times such that for each n, the evolution time t_1 is incrementally increased by an addition of a time equal to 1/bandwidth. Because of the dephasing that occurs during t_1, the signal occurs as an echo in the t_2 domain and with each increment in t_1, that echo appears at later times with decreasing intensity, a consequence of molecular diffusion, even at the shortest exchange time, τ_m. Nonetheless, the echo is always captured in the acquisition window and the attenuation effect leads to some broadening of the spectrum in the f_1 Fourier domain. However, once the exchange time is increased, the broadening grows significantly as molecules migrate to positions in which the local fields substantially differ. It is the growth of off-diagonal intensity, as a function of mixing time τ_m, which we exploit in these measurements.

The pulse sequence of Fig. 1 produces an $n \times m$ data matrix where m is given by the number of acquisition points. From here we apply a 2D Fourier transform to obtain the 2D frequency spectra shown in the next section. Data was processed using Matlab (The MathWorks, Natick, MA). Samples used were two randomly packed monodisperse glass beads (Duke Scientific Products, Fremont, CA) with diameters of 100 and 10 μm. The 100 μm beads were soda lime glass and the 10 μm beads were borosilicate glass.

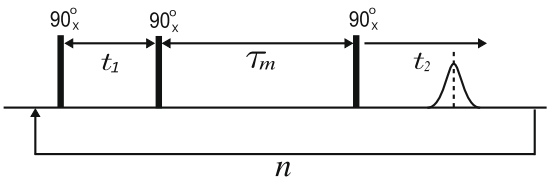

Fig. 1. 2D Pulse sequence used for local field exchange experiment. The evolution time, t_1, is increased incrementally for each n. The mixing time, τ_m, is kept constant for each repetition, but varies for each experiment.

3. Results and discussion

3.1. One hundred micrometers bead pack

3.1.1. 400 MHz

The 1D spectrum of the 100 μm bead pack at 400 MHz is shown in Fig. 2a. Full line width at half maximum (FWHM) is roughly 5.2 kHz. Taking the characteristic length to be the bead diameter, d, $d^2\delta\omega/D \approx 2 \times 10^4$.

For the 100 μm bead pack, 8 mixing times ranging from 1 to 640 ms were employed. We were unable to use longer mixing times due to decreased signal-to-noise ratio. Fig. 3 shows the 2D spectra obtained using 256 data points at 20 kHz acquisition and evolution bandwidths. The longest evolution time is thus 12.8 ms, corresponding to a diffusion length of around 7 μm. Note that each 2D spectrum has been normalised to constant total intensity so as to remove T_1 relaxation effects. We note that unlike [13], the 2D spectra obtained here are very symmetric.

A clear growth of off diagonal intensity is observed as the mixing time is increased. This growth is evident as a broadening of the 2D spectrum in the off-diagonal direction. This line broadening can be quantified by taking an average of two intensities located at equidistant points from the center peak, corresponding to frequency offsets comparable to the inhomogeneous linewidth. In Fig. 4 these intensities are plotted against mixing time. The error bars are estimated by consideration of noise in the system. We have repeated these measurements of off-diagonal intensity versus mixing time for a range of frequency offsets: 0.67, 0.83, 1.0 and 1.3 FWHM. In each case we fit the data to a bi-exponential growth relation $a_0 + a_1\exp(\frac{-t}{\tau_1}) + a_2\exp\left(\frac{-t}{\tau_2}\right)$. While the precision of the data justify a fit to more than one exponential, we acknowledge that a bi-exponential model may be simplistic and that a continuum of characteristic times may exist. Table 1 shows the values of the parameters obtained. There is a remarkable consistency of behaviors for whatever frequency offset is chosen for the analysis. In particular, we find characteristic times of $\tau_1 \approx 9$–20 ms and $\tau_2 \approx 250$–750 ms, the short time component (a_1) dominates at smaller offsets and the long time constant component (a_2) dominates at large offsets. Note that the τ_1 and τ_2 time constants correspond roughly with diffusive distances of 0.06–0.09 and 0.32–0.55 bead diameters, respectively, or to dimensionless time τ_1/τ_D and τ_2/τ_D 0.004–0.009 and 0.11–0.35 where τ_D is the time for a water molecule to diffuse one bead diameter.

Note that at lower intensity levels in the 2D spectra of Fig. 3, there is a ridge of intensity along the f_1 and f_2 axes, suggesting the presence of weak signals encoded only in a single frequency domain. These may be artifacts of the pulse sequence but their similar intensity in the evolution and acquisition domains suggest that they are a real feature of the data.

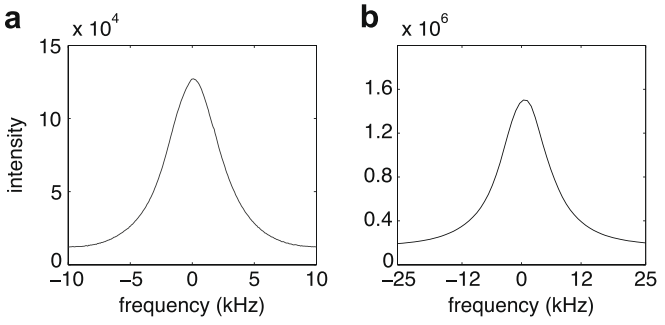

Fig. 2. (a) 1D ^{1}H NMR spectra obtained from water in 100 μm bead pack at 400 MHz with a 20 kHz bandwidth. (b) as for (a) but for 900 and 200 kHz bandwidth.

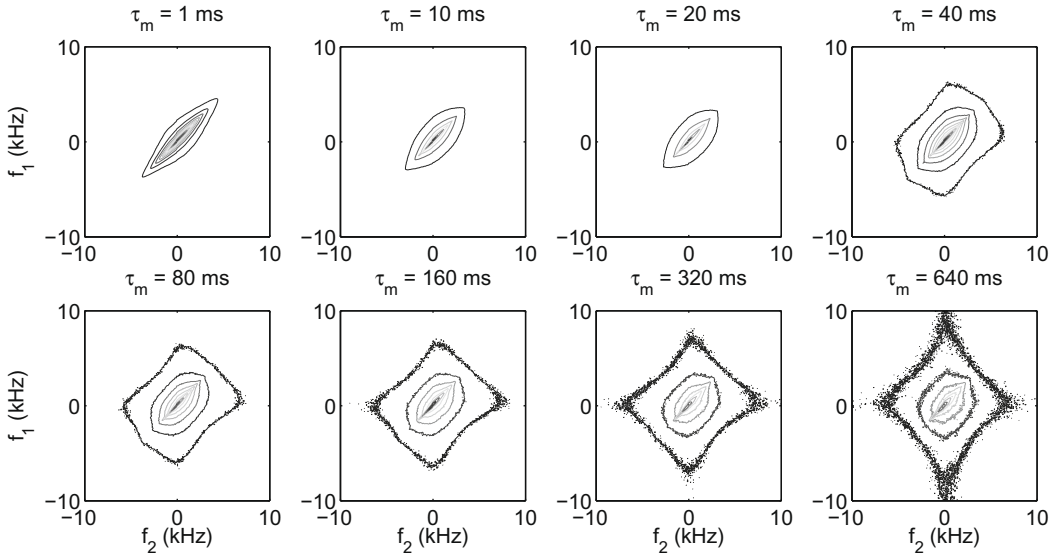

Fig. 3. 2D ^{1}H NMR exchange spectra obtained from water in 100 μm bead pack at 400 MHz with a 20 kHz bandwidth. The 8 examples show mixing times ranging from 1 to 640 ms.

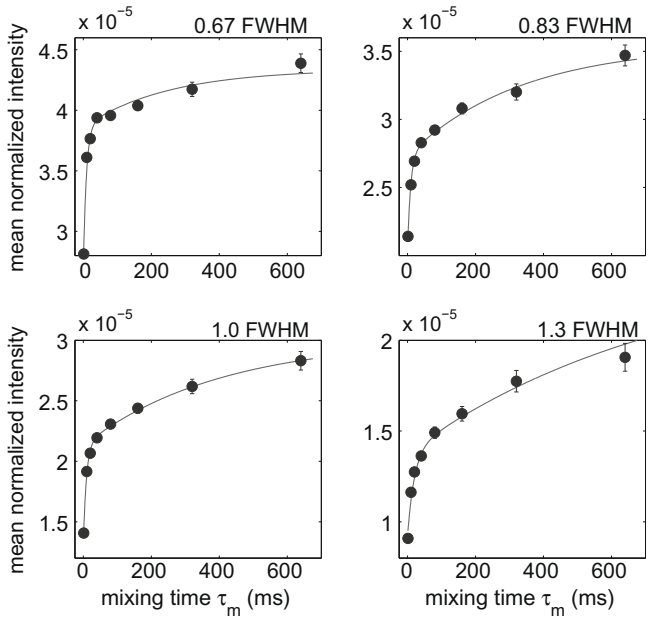

Fig. 4. Mean normalized intensities located at equidistant points of the center peak along the off-diagonal of spectra shown in Fig. 3 with respect to mixing time. The solid line is a fit to a bi-exponential growth $a_0 + a_1 \exp\left(\frac{-t}{\tau_1}\right) + a_2 \exp\left(\frac{-t}{\tau_2}\right)$.

Table 1
Parameters obtained for Fig. 4 with the bi-exponential growth relation $a_0 + a_1 \exp(\frac{-t}{\tau_1}) + a_2 \exp\left(\frac{-t}{\tau_2}\right)$. τ_D is the time required to diffuse one bead diameter.

	0.67 FWHM	0.83 FWHM	1.0 FWHM	1.3 FWHM
a_0	4.4×10^{-5}	3.6×10^{-5}	3×10^{-5}	2.4×10^{-5}
a_1	-1.1×10^{-5}	-6.7×10^{-6}	-8×10^{-6}	-4.5×10^{-6}
a_2	-4.8×10^{-6}	-8.2×10^{-6}	-8.8×10^{-6}	-1.1×10^{-5}
τ_1	9.1 ms	9.1 ms	9.1 ms	20.0 ms
τ_2	250 ms	330 ms	400 ms	770 ms
τ_1/τ_D	0.004	0.004	0.004	0.0092
τ_2/τ_D	0.12	0.15	0.18	0.23

3.1.2. 900 MHz

For the 900 MHz experiments, evolution and acquisition bandwidth was increased by an order of magnitude to 200 kHz while n was increased to 512 for a maximum t_1 of less than 3 ms, helping minimize the maximum diffusion distance during the evolution time to around 3 μm. Mixing times cover a range from 1 to 640 ms. Fig. 2b shows the 1D spectrum and Fig. 5 shows the 2D spectra obtained. Even though the bandwidth is 200 kHz, these figures show a bandwidth of 40 kHz to better display the spectra. The FWHM 1D spectrum is approximately, 11.8 kHz, which is roughly 9/4 broader than the 1D spectrum at 400 MHz, yielding $d^2\delta\omega/D \approx 5\times10^4$. All 2D spectra are normalized with respect to total intensity.

One of the most noticeable qualities of the 900 MHz data is the improved signal-to-noise ratio at longer mixing times. As with the 400 MHz data, we see a growth of off-diagonal intensity as mixing time is increased indicated by a line broadening in the off-diagonal direction. We quantify this broadening by taking the mean intensity of two points equidistant from the center peak, again at a frequency offset equal to the inhomogeneous linewidth. These mean intensities are shown in Fig. 6 along with a fit to the bi-exponential growth model.

The bi-exponential growth observed here is similar to that obtained from the 400 MHz experiments. Mean intensities are greater for the 900 MHz results than the 400 MHz results due to the higher signal to noise ratios at magnetic field. Characteristic bi-exponential growth times are again on the order of 10 and 500 ms. These correspond to water molecule diffusion of 0.07 and 0.45 bead diameters, respectively, and to τ_1/τ_D and τ_2/τ_D of 0.004 and 0.23, respectively.

3.2. Simulations

We now turn to a description of exchange in the inhomogeneous field based on computer simulations. For this purpose we utilized a random monodisperse bead obtained by dropping spheres one by one in a cylinder of diameter 10 bead diameters, allowing them to find their potential energy minimum. For the simulation, 511 spheres were used, packed to a height of 7 bead

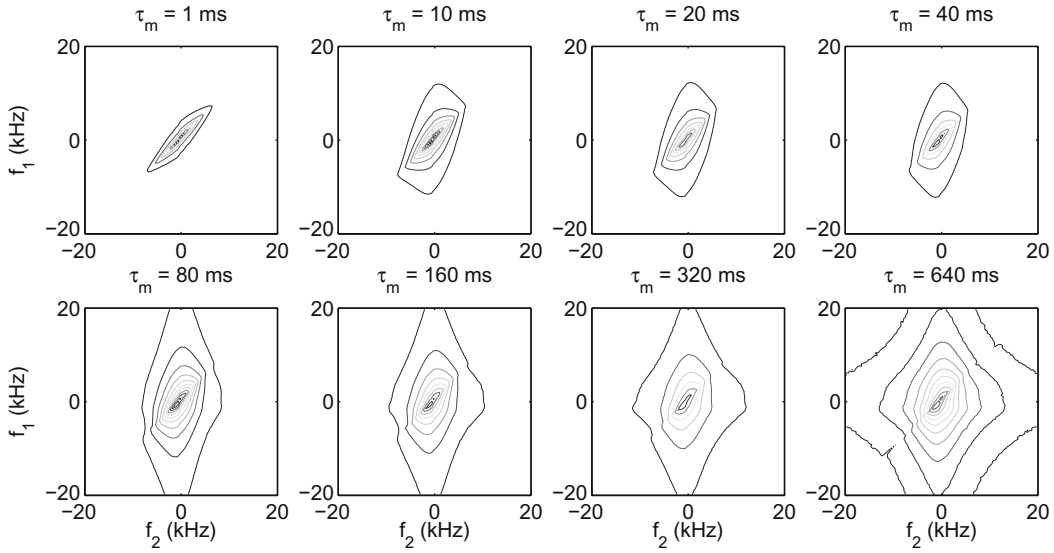

Fig. 5. 2D ^{1}H NMR exchange spectra obtained from water in 100 μm bead pack at 900 MHz with a 200 kHz bandwidth. The bandwidth shown is 40 kHz. The 8 examples show mixing times ranging from 1 to 640 ms.

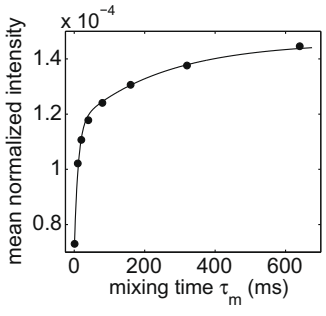

Fig. 6. Mean normalized intensities located at equidistant points of the center peak along the off-diagonal of spectra shown in Fig. 5 with respect to mixing time. The solid line is a fit to bi-exponential growth $a_0 + a_1 \exp\left(\frac{-t}{\tau_1}\right) + a_2 \exp\left(\frac{-t}{\tau_2}\right)$. The error bars in this case are smaller than the data markers.

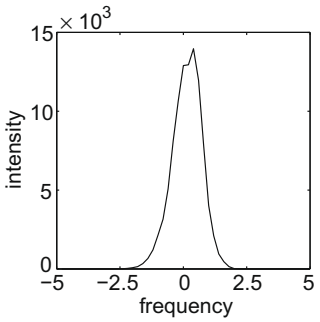

Fig. 7. Calculated NMR spectrum in dimensionless frequency units based on the 511 sphere random bead back. The spectrum is centred at slightly positive frequencies because the pack has unequal transverse and longitudinal dimensions with respect to the magnetic field.

diameters. The porosity of the bead pack was determined to be 43%. Using a mesh size of 0.0375 bead diameters, particles in a volume were allowed to diffuse on the grid by a Monte Carlo process involving reflection at bead surfaces. An initial particle volume of comprising a cube of side length 2.3 sphere diameters centered in the pack was used, the diffusion coefficient being determined by a 1-D rms hopping distance of 1 mesh element per dimensionless time unit (.000703 squared bead diameters/time unit). Initially, local magnetic field offset values were assigned to each particle by summing the contributions from all spheres in the pack, assuming a dipole at each sphere center, the particles then being allowed to diffuse for a set time before recalculating the local field offset assignments based on the final positions. Because the encoding for field is instantaneous for the initial and final position sets, the issue of motional averaging does not arise and so the absolute size of the field offsets in relation to any characteristic time for encoding is irrelevant. We have assumed a bead magnetization value of 3 dimensionless units for the purpose of our calculation.

Fig. 7 shows the calculated NMR spectrum for the initial particle positions. Note that the spectrum is centred at slightly positive frequencies, an effect due to the fact that the bead pack has unequal transverse and longitudinal dimensions with respect to the magnetic field. The FWHM is 1.2 dimensionless frequency units. Our simulation assumes the slow motion limit $d^2\delta\omega/D \to \infty$. Fig. 8 shows the manner in which the 2D exchange spectra evolve with increasing mixing time while Fig. 9a shows the growth of off-diagonal intensity taken from these 2D spectra by selecting the intensity at a frequency lying at off-diagonal frequency coordinates $(-0.8, 0.8)$ where 0.8 frequency units represents 0.67 FWHM.

The simulated data shown in Fig. 9 a is somewhat noisy and have been fitted with a simple single exponential growth curve. The growth rate corresponds to a time constant of around 44 dimensionless time units or a τ/τ_D of 0.061 making a 1D diffusion distance of 0.25 bead diameters. This is intermediate between the short and long time constants of the experiments. However, in the case of the simulations, we note that the time constant observed depends strongly on the frequency offset chosen for the analysis. Fig. 9b shows the dependence of the time constants for both simulated (τ/τ_D) and experimental (100 μm beads, τ_1/τ_D and τ_2/τ_D) on chosen frequency offset at which the off-diagonal intensity is measured. It is apparent that the experimental data, when fitted to a bi-exponential shows a degree of offset dependence for the fast component while the slow component increases with increasing offset. That the simulated and experiment do not agree is not surprising given that the simulations have not allowed for diffusion during the t_1 and t_2 encoding periods. Nor does the simulation account for the potential loss of signal from those spins experiencing more rapid T_1 relaxation. Nonetheless the simple computer model employed here gives some insight regarding the exchange process and broadly captures qualitative features of the data.

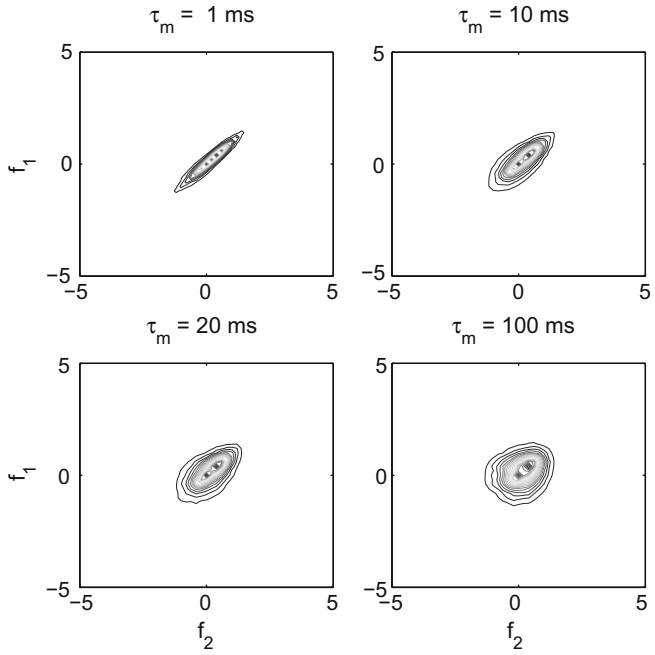

Fig. 8. Two dimensional exchange spectra calculated in the computer simulations. The dimensionless times of τ_m 1, 10, 20 and 100, correspond to diffusion distances of 0.04, 0.12, 0.13, and 0.38 bead diameters, respectively.

3.3. Ten micrometers bead pack

For porous media for which the slow limit, $l^2\delta\omega/D \gg 1$, does not apply, frequency exchange during the encoding periods t_1 and t_2 will lead to severe broadening of the 2D spectra even at the shortest mixing times employed. Nonetheless, the effect of an increasing mixing time may be sufficient to slightly enhance this broadening in the case where extreme motional averaging does not apply. For that reason we have attempted to carry our 2D exchange experiments for beads of 10 μm diameter. The diffusion distances at longest evolution time, 7 and 3 μm, for 400 and 900 MHz, correspond to a significant fraction of one bead diameter.

3.3.1. 400 MHz

The 1D spectrum for the 10 μm bead pack at 400 MHz gives a half height width of 2.7 kHz, smaller than that seen for the 100 μm beads presumably due to a different diamagnetic susceptibility for this particular glass. Here $d^2\delta\omega/D \approx 10^2$.

For the 10 μm bead pack, 12 mixing times are employed ranging from 1 to 40 ms. The smaller range of mixing times is needed because it takes less time for a water molecule to diffuse through the smaller pore space in the 10 μm bead pack compared to the larger pore space of the 100 μm bead pack. The resultant spectra can be seen in Fig. 10. These 2D spectra have also been normalized to constant total intensity in order to remove T_1 relaxation effects. Because of the rapid motional averaging occuring during the frequency encoding times, the 2D spectra are very broad, even at the shortest mixing time. Consequently, the growth of off-diagonal spectral characteristics is not as noticeable as found for the 100 μm beads. The shortest mixing time lacks a sharply diagonal spectrum. Even during the 1 ms mixing time, significant diffusion has taken place compared to that for the 100 μm sample. Nonetheless, some additional broadening is visible over mixing times from 1 to 20 ms, just enough for us to be able to observe pore exchange effects. This residual visibility results from the fact that it takes about 25 ms for a water molecule to diffuse one bead diameter. The line broadening can again be quantified by taking the average of two intensities at equidistant points from the center peak and plotting them against mixing time, shown in Fig. 11. Again we see a growth, albeit over a shorter time scale than that of the 100 μm bead pack.

3.3.2. 900 MHz

The same 12 mixing times were used for the 10 μm sample at 900 MHz at a bandwidth of 200 kHz and an n of 512. The maximum t_1 for the 900 MHz experiments is less than 3 ms, comparable to a 3–4 μm diffusion distance. The 1D spectrum has a FWHM of roughly 6.2 kHz. The 2D spectra are shown in Fig. 12. All spectra have been plotted with a display bandwidth of 40 kHz rather than their full 200 kHz to better observe the broadening with respect to increasing mixing time. All 2D spectra have been normalized with respect to integrated intensity to compensate for T_1 relaxation over the mixing time. Most noticeable in comparing the 400 and 900 MHz spectra is the decrease in noise due to the higher magnetic field. Off-diagonal broadening indicates an increase in off-diagonal intensity. Quantification of this intensity with respect to mixing time is shown in Fig. 11.

The growth of off-diagonal for the 10 μm beads at 900 MHz shows a trend similar to that found for 10 μm at 400 MHz. In both cases characteristic times of 2 ms and 20–50 ms, corresponding to 0.2 and 1 bead diameters. However, given the large amount of exchange which occurs during the encoding periods, we are cautious in attributing significance to these parameters.

4. Experimental

The experiments were performed using Bruker 400 and 900 MHz spectrometers and the proton NMR signal from water imbibed in a randomly packed matrix of monodisperse glass spheres.

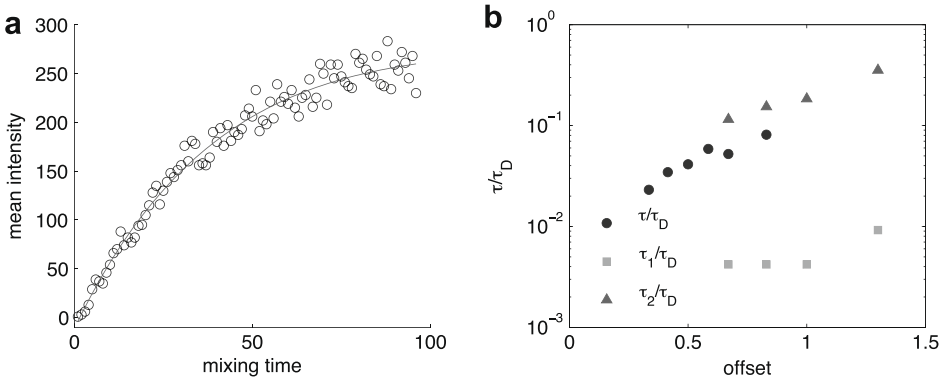

Fig. 9. (a) Growth of off-diagonal intensity at 0.67 FWHM frequency off-set as a function of dimensionless mixing time, obtained from simulated 2D exchange spectra for a random bead pack. The solid line represents a single exponential fit curve. (b) τ/τ_D as a function of frequency offset as a fraction of FWHM for both the simulated (solid circles) and experimental data (solid squares and triangles).

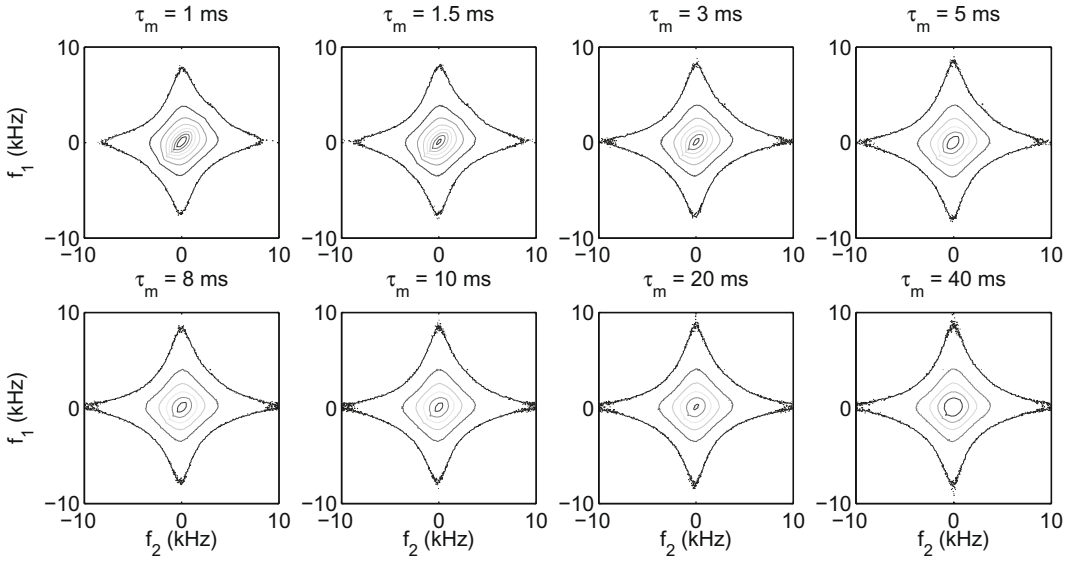

Fig. 10. 2D ^{1}H NMR exchange spectra obtained from water in 10 μm bead pack at 400 MHz with a bandwidth of 20 kHz. The 12 examples show mixing times ranging from 1 to 40 ms.

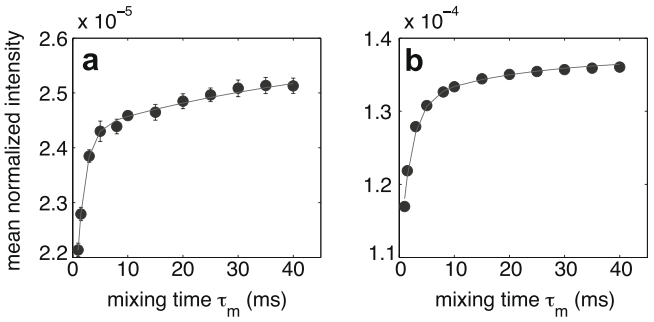

Fig. 11. (a) Mean normalized intensities located at equidistant points of the center peak along the off-diagonal of 400 MHz spectra shown in Fig. 10 with respect to mixing time. The solid line is a fit of bi-exponential growth. (b) as for (a) but for 900 MHz.

Specifically, two different samples of monodisperse glass beads (Duke Scientific Products, Fremont, CA) were used. These had diameters of 100 and 10 μm and a standard deviation of 3.6 and 1.5 μm, respectively. Different ranges of mixing times were used for each sample depending on bead size. At 400 MHz, the bandwidth in both the evolution and detection periods is 20 kHz, with 256 data points being acquired. This leads to a total evolution time less than 13 ms, thus ensuring the diffusive motion of water molecules during the encoding times is much smaller than the bead size in the 100 μm sphere diameter case, and comparable with the sphere size in the 10 μm case. Each experiment took roughly 45 min to run with both n and $m = 256$.

For comparison, experiments were also performed on a Bruker 900 MHz spectrometer at the University of Queensland in Australia. The higher magnetic field and greater inhomogeneous linewidth allowed us to increase the bandwidth, resulting in a shorter evolution time during frequency encoding. Temperature was held constant at 25 °C for all experiments.

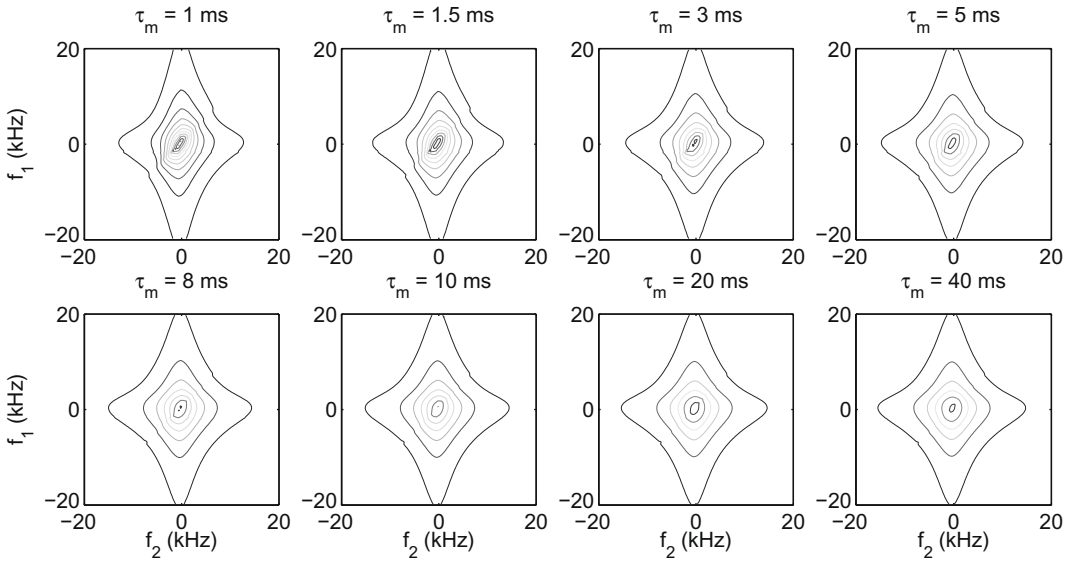

Fig. 12. 2D ^{1}H NMR exchange spectra obtained from water in 10 μm bead pack at 900 MHz with a bandwidth of 200 kHz. Bandwidth shown in the figure is 40 kHz. The 12 examples show mixing times ranging from 1 to 40 ms.

5. Conclusions

The results presented here show that it is possible to use a 2D Fourier transformation of a simple evolution–storage–exchange experiment to reveal diffusive migration of molecules through the pore space. A key aspect of the method is the use of large polarizing fields, sufficient to give a field inhomogeneity frequency spread wide enough to keep the frequency encoding time much less than the time taken to diffuse one pore. Nontheless the method is applicable to lower fields, provided that susceptibility inhomogeneity is sufficiently large, as judged by the criterion $l^2\delta\omega/D \gg 1$. However, we have shown here that even when this criterion is relaxed, significant exchange effects are observable.

The experiments performed here have employed random monodisperse bead packs for which computer simulations have been performed. In the experiments, an apparent bi-exponential growth of off-diagonal intensity is observed. The fast time constant corresponds to a diffusion distance of around 0.1 bead diameters, while the second is on the order of 0.5 bead diameters a result which depends only weakly on the choice of frequency offset. Bi-exponential behavior suggests length scale complexity, probably reflecting the rather unusually shaped pore space of random sphere packs though we acknowledge that a broad distribution of characteristic times is more likely. The computer simulation showed time constants correspond to characteristic lengths different from those observed in the experiment. There are a number of reasons why the simple simulation model employed here may not precisely represent the experimental conditions. Nonetheless we are able to see that in both experiment and simulation characteristic times reflect diffusion on the order of 0.1–0.3 pore diameters, enough to give a fair indication of pore size.

Naturally we would be interested to test the method in different porous substances, for example, sandstones. The exchange demonstrated here is but one example of the potential uses of the multi-dimensional approach using susceptibility-induced field inhomogeneity, ΔB_0. One especially interesting application is the combination of encoding for local field, with other parameters requiring an inverse Laplace analysis, Examples would be ΔB_0 vs T_2 correlation, ΔB_0 vs D correlation and ΔB_0 vs g^2. The latter is of particular interest because local gradients depend on spatial derivatives of the field inhomogeneity. Correlating ΔB_0 with $\nabla \cdot \Delta B_0$ provides an interesting probe of structural geometry.

Acknowledgments

The authors are grateful to the New Zealand Foundation for Research, Science and Technology NERF funding program, and to the Queensland NMR network for allowing us use of their 900 MHz NMR machine.

References

[1] E.O. Stejskal, J.E. Tanner, Spin diffusion measurements: spin echoes in the presence of a time-dependent field gradient, Journal of Chemical Physics 42 (1) (1965) 288–292.
[2] Y.-Q. Song, S. Ryu, P.N. Sen, Determining multiple length scales in rocks, Nature 406 (6792) (2000) 178–181.
[3] P.J. McDonald, J.-P. Korb, J. Mitchell, L. Monteilhet, Surface relaxation and chemical exchange in hydrating cement pastes: a two-dimensional NMR relaxation study, Physical Review E 72 (2005).
[4] K.E. Washburn, P.T. Callaghan, Tracking pore to pore exchange using relaxation exchange spectroscopy, Physical Review Letters 97 (17) (2006) 175502/1-4.
[5] L. Venkataramanan, Y.Q. Song, M.D. Hurlimann, Solving fredholm integrals of the first kind with tensor product structure in 2 and 2.5 dimensions, IEEE Transactions On Signal Processing 50 (5) (2002) 1017–1026.
[6] J.H. Lee, C. Labadie, C.S. Springer, G.S. Harbison, Two-dimensional inverse laplace transform NMR: altered relaxation times allow detection of exchange correlation, Journal of the American Chemical Society 115 (17) (1993) 7761–7764.
[7] Y.Q. Song, L. Venkataramanan, M.D. Hurlimann, M. Flaum, P. Frulla, C. Straley, t1–t2 Correlation spectra obtained using a fast two-dimensional laplace inversion, Journal Of Magnetic Resonance 154 (2) (2002) 261–268.
[8] M.D. Hurlimann, L. Venkataramanan, Quantitative measurement of two-dimensional distribution functions of diffusion and relaxation in grossly inhomogeneous fields, Journal of Magnetic Resonance 157 (2002) 31–42.
[9] P.T. Callaghan, I. Furo, Diffusion–diffusion correlation and exchange as a signature for local order and dynamics, Journal of Chemical Physics 120 (8) (2004) 4032–4038.
[10] B. Sun, K.J. Dun, Probing the internal field gradients of porous media, Physical Review E 65 (5) (2002) 051309/1-7.
[11] J.G. Seland, K.E. Washburn, H.W. Anthonsen, J. Krane, Correlations between diffusion, internal magnetic field gradients, and transverse relaxation in porous systems containing oil and water, Physical Review E 70(5) (2004) 051305/1–10.
[12] S. Godefroy, P.T. Callaghan, 2d relaxation/diffusion correlations in porous media, Magnetic Resonance Imaging 21 (3–4) (2003) 381–383.
[13] J.-F. Kuntz, P. Palmas, V. Level, D. Canet, Restricted diffusion and exchange of water in porous media: average structure determination and size distribution resolved from effect of local field gradients on the proton NMR spectrum, Journal of Magnetic Resonance 191 (2008) 239–247.
[14] R.J. Brown, Distribution of fields from randomly placed dipoles—freeprecession signal decay as result of magnetic grains, Physical Review 121 (5) (1961) 1379–1382.
[15] L.E. Drain, Broadening of magnetic resonance lines due to field inhomogeneities in powdered samples, Proceedings of the Physical Society of London 80 (518) (1962) 1380.
[16] B. Audoly, P.N. Sen, S. Ryu, Y.-Q. Song, Correlation functions for inhomogeneous magnetic field in random media with application to a dense random pack of spheres, Journal of Magnetic Resonance 164 (2003) 154–159.
[17] Q. Chen, A.E. Marble, B.G. Colpitts, B.J. Balcom, The internal magnetic field distribution, and single exponential magnetic resonance free induction decay, in rocks, Journal Of Magnetic Resonance 175 (2) (2005) 300–308.
[18] J. Jeener, B.H. Meier, P. Bachmann, R.R. Ernst, Investigation of exchange processes by two-dimensional NMR spectroscopy, Journal of Chemical Physics 71 (1979) 4546–4553.